Carcinogenesis vol.34 no.2 pp.415–425, 2013
doi:10.1093/carcin/bgs329
Advance Access publication October 24, 2012

miR-18a promotes malignant progression by impairing microRNA biogenesis in nasopharyngeal carcinoma

Zhaohui Luo[1–3], Yafei Dai[2], Liyang zhang[2], Chen Jiang[2], Zheng Li[2], Jianbo Yang[4], James B. McCarthy[4], Xiaoling She[5], Wenling Zhang[1], Jian Ma[1], Wei Xiong[1], Minghua Wu[1], Jianhong Lu[1], Xiayu Li[1], Xiaoling Li[1], Juanjuan Xiang[1,2,*] and Guiyuan Li[1,2]

[1]Hunan Key Laboratory of Nonresolving Inflammation and Cancer, Changsha, Hunan 410013, China, [2]Cancer Research Institute, Key Laboratory of Carcinogenesis and Cancer Invasion of Ministry of Education, Key Laboratory of Carcinogenesis of Ministry of Health, Central South University, 110 Xiangya Road, Changsha, Hunan 410078, China, [3]Department of Neurology, Xiangya Hospital, Central South University, Changsha, Hunan 410008, China, [4]Department of Laboratory Medicine and Pathology, University of Minnesota Masonic Cancer Center, Minneapolis, MN, USA and [5]Department of Pathology, Second Xiang Ya Hospital, Central South University, Changsha, Hunan 410011, China

*To whom correspondence should be addressed. Tel: +0086-731-82355401; Fax: +0086-731-82355401;
Email: xiangjj@csu.edu.cn
Correspondence may also be sent to Guiyuan Li. Tel: +0086-731-84805383; Fax: +0086-731-84805383;
Email: ligy@xysm.net

Dysregulation of microRNA (miRNA) biogenesis is implicated in cancer development and progression. Dicer and Drosha are established regulators of miRNA biogenesis. In this study, we used a miRNA array to evaluate the miRNA expression profiles in nasopharyngeal carcinoma (NPC) samples. The significance analysis of microarrays showed a global downregulation of miRNA expression in NPC samples compared with normal nasopharyngeal epithelial tissues. Notably, miR-18a, a member of the oncogenic miR-17–92 cluster, was upregulated in the NPC samples and ell lines. Clinical parameter studies showed that higher levels of miR-18a correlated with NPC advanced stage, lymph node metastasis, Epstein-Barr virus infection and a higher death rate from NPC, indicating oncogenic roles in NPC development. The expression levels of miR-18a and Dicer1 were inversely related in NPC tissues. Further studies demonstrated that miR-18a negatively regulated Dicer1 by binding to the 3′ untranslated regions of Dicer1. *In vitro* and *in vivo* biological function assays showed that miR-18a promoted the growth, migration and invasion of NPC cells by regulating Dicer1 expression, which caused the global downregulation of miRNA expression levels including miR-200 family and miR-143. Furthermore, we found that the epithelial mesenchymal transition marker E-cadherin and the oncogene K-Ras were aberrantly expressed after miR-18a transduction, and these alterations were directly induced by downregulation of the miR-200 family and miR-143. Collectively, our findings indicate that miR-18a plays an oncogenic role in the development of NPC by widespread downregulation of the miRNome and could be a potential therapeutic target for NPC.

Introduction

MicroRNAs (miRNAs) are small non-coding RNAs that are 20–22 nucleotides in length. Since the first miRNA was identified in 1993, miRNAs have been widely reported to be involved in cancer initiation and development. In 2005, miRNAs' expression profiling studies were performed in human samples including cancer tissues (1). Although several miRNAs are upregulated in specific tumours, widespread deregulation of miRNA expression has been found in human cancers (1–4). Of note, the upregulation of the miR-17–92 cluster in various types of cancer implied an oncogenic role in the occurrence and progression of cancer (5–7). However, miR-18a, a member of the miR-17–92 cluster, was instead reported to suppress cell proliferation in bladder cancer T24 cells (8). On the other hand, it was reported that ERalpha binds to c-MYC and in turn upregulates the expression of pre-miR-18a in an oestrogen-dependent manner, suggesting an oncogenic role for miR-18a in breast cancer (9). Recently, the diagnostic value of circulating miR-18a in plasma was reported for pancreatic cancer (10). Therefore, miR-18a may play different roles in various types of cancer through different targeted genes.

Research on nasopharyngeal carcinoma (NPC) has mirrored other cancer research programs. The research has focused largely on molecular defects including the dysregulation of miRNAs. To date, several miRNAs have been shown to target specific mRNAs to regulate the progression of NPC. miR-216b (11), miR-218 (12), miR-26a/b (13,14), miR-10b (15), let-7 (16), miR-141 (17) and miR-200a (18) have been shown to have tumour-suppressive functions in NPC. Not surprisingly, Epstein-Barr virus (EBV)-encoded miRNAs have oncogenic properties (19–21). In addition, other miRNAs such as miR-155, enhanced by EBV-encoded LMP1 and LMP2A, are associated with poor prognosis in NPC patients (22). miRNA expression profiling also confirmed the widespread downregulation of miRNAs in NPC samples compared with the histologically normal nasopharyngeal epithelial tissue (23–25). In these miRNA expression profile studies, miR-18a was shown to be upregulated. Our previous data also demonstrated that miR-18a showed significant upregulation during NPC progression (26), suggesting an oncogenic role for miR-18a in NPC.

Dicer is a member of the double-stranded RNA-specific ribonuclease III family that is required for RNA processing and degradation (27). The expression of Dicer in different cancers varies (28). Dicer is over-expressed in prostate cancer (29); however, Dicer also appears to play a tumour-suppressive role. Cancer specimens with both high Dicer expression and high Drosha expression are associated with increased median survival in ovarian cancer patients (30). Our previous work demonstrated a significant downregulation of Dicer in NPC biopsies compared with normal counterparts (31).

In this study, we aimed to examine the roles of miR-18a in the progression of NPC and, importantly, to clarify the mechanism by which miR-18a promotes malignant tumour progression. Efforts to interpret the association of miR-18a and Dicer are included in this report.

Materials and methods

Cell lines

NPC cell lines including 5-8F, 6-10B, HK1, HNE1, HNE2, HONE1,CNE1,CNE2 and 293FT were cultured in RPMI-1640 medium supplemented with penicillin G (100 U/ml), streptomycin (100 mg/ml) and 10% foetal calf serum. Immortalized normal nasopharynx epithelial NP69 cells were cultured in RPMI-1640 medium supplemented with penicillin G (100 U/ml), streptomycin (100 mg/ml), 10% foetal calf serum and growth factors. The cells were grown at 37°C in a humidified atmosphere of 5% CO_2 and were routinely sub-cultured using 0.25% (w/v) trypsin–ethylenediaminetetraacetic acid solution.

Vectors, oligonucleotides and antibodies

Synthetic miRNA mimics and 2′-O-methyl-modified inhibitors 'antagomiRs' were purchased from Genepharma Company, Shanghai, China. An miR-insensitive Dicer1 construct was purchased from Genecopoeia Company, Guangzhou, China. The miR-18a, miR-18a inhibitor and scramble control lentivirus were purchased from SunBio Company, Shanghai, China. Rabbit–anti-human E-cadherin antibody, rabbit–anti-human K-Ras antibody and

Abbreviations: ANOVA, analysis of variance; EBV, Epstein-Barr virus; EMT, epithelial mesenchymal transition; GAPDH, glyceraldehyde 3-phosphate dehydrogenase; LNA, locked nucleic acid; miRNA, microRNA; MTT, 3-(4,5-dimethylthiazole-2-yl)-2,5-diphenyl tetrazolium bromide; NPC, nasopharyngeal carcinoma; PBS, phosphate-buffered saline; qPCR, quantitative PCR; RT–PCR, reverse transcription–PCR; SD, standard deviation; UTR, untranslated regions; RIPA buffer, Radio-Immunoprecipitation Assay Buffer.

rabbit–anti-human Dicer1 antibody were purchased from Cell Signaling Technology Inc.

Quantitative real-time PCR

Expression of the miRNAs was evaluated using SYBR green quantitative real-time reverse transcription (RT)–PCR (Takara, China). Total RNA was extracted using Trizol® reagent (Invitrogen) from cells and samples. The individual microRNA qPCR Quantitation kit was purchased from Genepharma Company, China. The quantitative PCR (qPCR) was performed according to the instructions. The qPCR cycle was 98°C for 2 min and 40 cycles of 95°C for 15 s and 60°C for 30 s. The final melting curve analysis (60°–95°C) was included. The standard curve was produced with slopes at approximately −3.32 (~100% efficiency); the miRNA PCR quantification used the $2^{\Delta\Delta Ct}$ method against U6 for normalization. Messenger RNA PCR quantification used the $2^{\Delta\Delta Ct}$ method against glyceraldehyde 3-phosphate dehydrogenase (GAPDH) for normalization. The data are representative of the means of three experiments. RT–PCR primers are listed in Supplementary Table 1, available at *Carcinigenesis* Online.

MTT assay

The cells were seeded at a density of 2×10^3 cells/well in 96-well plates 24 h before transfection. The cells were incubated in growth medium for 24 h. A volume of 20 µl of 3-(4,5-dimethylthiazole-2-yl)-2,5-diphenyl tetrazolium bromide (MTT) solution (5 mg/ml) was added to each well. The plate was incubated at 37°C for an additional 4 h. The media were removed and 150 µl of dimethyl sulfoxide was added to each well. The plates were shaken for 10 mins to dissolve the MTT formazan crystals. The optical density of each well was determined with a scanning multi-well spectrophotometer at a wavelength of 490 nm. The experiment was repeated three times; six parallel samples were measured each time.

Wound closure assay

The cells were transfected with the synthetic miRNA mimics or the 2′-O-methyl-modified inhibitors antagomiR-18a and grown to 90% confluency in a six-well dish. A wound was created using a sterile 10 µL pipette tip followed by a wash with 1× phosphate-buffered saline (PBS) to remove detached cells. Then, the cells were cultured in medium with 2% serum, and migration at the corresponding wound site was documented using a microscope (Nikon) at different time points (0, 24 and 48 h).

Transwell migration assay

Before cell seeding, Corning Costar Transwell 24-well plates (8 µm pores; Corning) were coated with Matrigel (BD) and placed in the cell culture hood for 1 h at 37°C. A total of 1×10^5 cells was seeded in the inserts after transfections and cultured in medium with 2% serum. Normal growth medium was placed in the bottom wells. The cells were then allowed to migrate for 24 or 48 h. The migrated cells were fixed with 100% methanol for 1 min and allowed to air dry. The invasive cells on the lower surface of the membrane were stained by dipping the inserts in a staining solution for 20 min and the stained cells were counted.

Western blot assay

The protein used for western blotting was extracted using Radio-Immunoprecipitation Assay Buffer (RIPA buffer) containing protease inhibitors (50 mM Tris, pH 7.4; 100 mM NaCl; 1% nonidet P-40; 0.5% deoxycholic acid; 0.1% sodium dodecyl sulphate; 10 µg/ml aprotinin; 10 µg/ml leupeptin;1 mM phenylmethylsulphonyl fluoride). The proteins were quantified using the BCA™ Protein Assay Kit (Pierce). The western blot system was established using a BioRad Bis-Tris Gel system according to the manufacturer's instructions (BioRad). The primary antibodies were prepared in 5% blocking buffer. The primary antibody (against Dicer1, E-cadherin or K-Ras) was incubated on the membrane overnight at 4°C followed by a brief wash and incubation with secondary antibody for 1 h at room temperature. Finally, a peroxide and luminol solution 40:1 was added to cover the blot surface for 5 min at room temperature. The signals were captured and the intensity of the bands was quantified using the BioRad ChemiDoc XRS system.

miRNA microarrays

Total RNA was extracted using Trizol® reagent (Invitrogen) from cells and samples. A total of 200 ng of total RNA from each sample was used for the follow-up microarray. Poly(A) polymerase was used to add a stretch of poly-A tail to the 3′ end of each sequence in total RNA. The Ambion Illumina TotalPrep RNA Amplification Kit was used to synthesize biotinylated complementary DNA. The PCR was performed using fluorescently labelled universal primers; then, the fluorescently labelled, single-stranded PCR products were hybridized to capture beads. The miRNA expression profiling kit contains primers for 1146 human miRNAs. The biotinylated complementary DNA was hybridized with miRNA-specific oligos. The unbound oligos were washed away followed by the extension and ligation reaction. The fluorescent signals were then detected using the Illumina iScan System. All steps were performed according to the manufacturer's instructions.

Immunohistochemistry and hybridization in situ

The NPC samples and normal nasopharyngeal tissues were fixed and embedded in paraffin wax. Paraffin sections 4–6 µm thick were dewaxed followed by hydration. The sections were then ready for immunohistochemistry and hybridization *in situ*. For immunohistochemistry, the sections were dipped into antigen retrieval buffer (0.01 M citrate buffer, pH 6.0) followed by microwave heating for 5 min. The tissue sections were rinsed with 0.01 M PBS, pH 7.4 and incubated with primary antibody (Dicer1, 1:50 dilution; Cell Signaling, USA) at 4°C overnight in a humidified chamber. After extensive washing with PBS, the sections were incubated with biotin-linked goat anti-rabbit IgG antibodies (UltraSensitive S-P Kit, Maixin Biotechnology Company, Fuzhou, China). For hybridization *in situ*, after being dewaxed and hydrated, the slides were transferred into a 3% H_2O_2 and protease buffer for inactivation of endogenous enzymes. The slides were then treated with pepsin diluted in 3% citric acid. The slides were hybridized overnight at 59°C with 50 nM DIG-labelled locked nucleic acid (LNA)-based probe specific for miR-18a or LNA-src-miR negative control probe (Exiqon, Vedbaek, Denmark). After rinsing, the sections were blocked in blocking buffer. An antibody specific for DIG-AP Fab fragments antibody was applied to the sections.

The above sections were then washed and developed using 3′-diaminobenzidine hydrochloride as the chromogen, and the sections were counterstained with haematoxylin. Finally, after dehydration and mounting, the sections were observed and imaged under a microscope (OLYMPUS BX-51, Japan). Goat serum and PBS were used in place of the primary antibody as a negative and blank control, respectively. A semi-quantitative scoring criterion for immunohistochemistry was used, in which both staining intensity and positive areas were recorded. Two pathologists independently assessed the immunohistochemistry and hybridization *in situ* scoring in the NPC tissue samples. Kappa statistics were used as measures of agreement between the different pathologists.

Luciferase assay

Luciferase activity was measured using the Dual-Glo luciferase assay system (Promega). Renilla luciferase activity was used to normalize the corresponding firefly luciferase activity.

Lentiviral vectors and cell transduction

HK1 cells stably expressing the GFP-luciferase were established using the ViraPower™ Lentiviral Expression System (Invitrogen) as described previously (32). Briefly, the coding sequence of the GFP fusion with luciferase was subcloned into pLenti6/V5-D-TOPO (Invitrogen). pLenti6/V5-DTOPO/GFP-luciferase and the ViraPower™ Packaging Mix (Invitrogen) were co-transfected using Lipofectamine 2000 (Invitrogen) into the 293FT cell line to produce a lentiviral stock. Forty-eight hours post-transfection, the virus-containing supernatant was harvested by collecting the medium. The viral particles were purified by ultracentrifugation through a 20% sucrose cushion. For infection of HK1 cells, the cells were cultured in six-well plates and when the culture reached 80% confluence, the concentrated lentivirus was added to the culture dishes. The stable-expressed GFP-luciferase HK1 cells were sorted using fluorescence-activated cell sorting (MoFlo, Beckman-Coulter,).

For the Dicer1 hairpin shRNA construct, oligos (5′-UCCAGAGCU GCUUCAAGCATT-3′ and 5′-UGCUUGAAGCAGCUCU GGATT-3′) were designed to construct the lentivirus gene transfer vectors (4). The double-stranded shRNA oligo was cloned into the BLOCK-iT™ lentivirus vector. The lentivirus vector was also cotransfected with the lentivirus package plasmids into 293FT cells. The infection procedures were described above.

Animal experiment and in vivo imaging of xenotransplanted NPC

The stable knockdown of miR-18a HK1 cells was achieved through infection of a lentivirus with miR-18a or miR-18a inhibitor into the GFP-luciferase HK1 cells. The cells were used for subcutaneous and metastatic tumour mouse models. Animal experiments followed protocols approved by Central South University. The cells were trypsinized with 0.25 M ethylenediaminetetraacetic acid and 0.05% trypsin (Invitrogen) on the day of transplantation and resuspended in PBS. The cells were injected subcutaneously or intravenously into nude mice. The animals were examined at different time points after the injection by measuring the size of subcutaneous tumour or by using the imaging system IVIS Lumina II. D-Luciferin was administered to each mouse by intraperitoneal injection at a dose of 150 mg/kg and the mice were anesthetized for 5 min in a chamber with 3% isofluorane. The mice were then imaged using a 20 cm field of view and an exposure time of 3 mins (3-min exposure; f-stop,1; binning,16; field of view,15 cm). The bioluminescence values were calculated by measuring photons/s/cm 2 /sr in the region of interest.

Clinical specimens

Human NPC specimens were collected from the Xiangya Second Hospital, Central South University, China. The patients were informed regarding the sample collection and they signed informed consent forms. The collections and use of tissue samples were approved by the Ethical Review Committee of Xiangya Second Hospital.

Statistical analysis

Survival data were analysed using Kaplan–Meier analyses. A log-rank test and χ^2-test were used to determine the difference among survival curves according to miR-18a status. The data including qRT–PCR and *in vivo* experiments are represented as the mean ± deviation. The Mann–Whitney *U*-test was used to compare the values of expression of Dicer1 and miR-18a at different NPC stages. Analysis of variance (ANOVA) was used for comparison of tumour volumes between groups.The intensity values from the microRNA array were analysed by significance analysis of microarray (SAM). The statistical analyses were performed using SPSS11.0. All *P* values were two-sided, and *P* values less than 0.05 were considered to be significant. Cronbach's alpha was calculated using SPSS to evaluate the agreement between two pathologists.

Results

Comparison between normal and NPC samples revealed global repression in miRNA expression

To investigate the global miRNAs expression profiles in nasopharyngeal carcinoma, we performed a miRNA microarray analysis of 12 NPC cases and 6 control samples of healthy nasopharyngeal epithelial tissues. Significance was determined using SAM (Figure 1A). As shown in Figure 1B, hierarchical clustering revealed two branches of non-random partitioning of the samples, normal and cancer samples, in which the observed distinct patterns of miRNA expression may reflect the mechanisms of NPC tumorigenesis. Although the expression levels of certain miRNAs were upregulated or unchanged, most of the miRNAs (141 out of 174) were downregulated in NPC samples compared with normal samples, implying an impairment of miRNA biogenesis process (Figure 1A).

The expression levels of Dicer1 and miR-18a are inversely related

As Dicer1 is an important established regulator of miRNA processing, the expression level of Dicer1 was evaluated using quantitative real-time PCR in 38 NPC samples and 10 normal nasopharyngeal epithelial tissues. We found that with the progression of NPC, the expression levels of Dicer1 decreased (Figure 1C, $P < 0.01$, two-sided Student's *t*-test). The expression levels of Dicer1 were clearly downregulated in NPC cell lines compared with the normal nasopharyngeal epithelial NP69 (Figure 1D). Immunohistochemistry was performed on 90 NPC samples and 23 normal control samples (Figure 1G). High expression levels of Dicer1 were detected in 82% of normal nasopharyngeal epithelial tissue (19 out of 23); significantly downregulated expression levels of Dicer1 were observed in 72% of NPC samples (65 out of 90).

Despite the widespread repression of miRNA in NPC, we noticed that the miR-17–92 cluster was upregulated in NPC samples compared with normal nasopharyngeal tissues (Figure 1B). We found that the expression levels of miR-18a, a member of the miR-17–92 cluster, were increased in the different clinical stages of NPC compared with the normal nasopharyngeal tissue. The expression levels of miR-18a were then confirmed using quantitative real-time PCR in the above-mentioned 38 NPC samples and 10 normal nasopharyngeal epithelial tissues. We found that with the progression of NPC, the expression levels of miR-18a increased. The higher levels of miR-18a significantly correlated with advancing stage (Figure 1E; $P < 0.01$, Mann–Whitney *U*-test). The expression levels of miR-18a were also examined in NPC cell lines, showing that miR-18a was clearly upregulated in NPC cell lines compared with the normal nasopharyngeal epithelial NP69 (Figure 1F). As shown, the expression levels of miR-18a were inversely related to the expression levels of Dicer1 in NPC samples and cell lines. The normal nasopharynx epithelial NP69 showed high levels of Dicer1 expression and low levels of miR-18a expression, whereas the NPC cell lines showed relatively low levels of Dicer1 expression and high levels of miR-18a.

In situ hybridization of miR-18a was then performed in 168 NPC samples. Collectively, the NPC specimens showed increased levels of miR-18a expression (Figure 1G). Staining was scored according to intensity and proportion (1.0–25%; 2.26–50%; 3.51–75%; 4.76–100%). The sum of intensity and percentage counts was used as the final score. We considered <8 as low expression and ≥8 as high expression (Table I). In the NPC patient samples, we also observed an inverse correlation of miR-18a and Dicer1 expression levels. Higher levels of miR-18a correlated with advanced stage, lymph node metastasis and EBV infection ($P < 0.01$) but were not associated with age and gender (Table I). The assessed histomical scores were in agreement in 90% of the samples. The cronbach's alpha statistics for concordance was 0.903 ($P < 0.0001$). To determine the survival differences according to the miR-18a expression levels, Kaplan–Meier plots were constructed ($n = 68$). Increased survival was associated with low expression levels of miR-18a (Figure 1H; hazard ratio, 0.4147; 95% CI, 0.2208–0.7791; $P = 0.0062$). These results indicated that high death rates from NPC were associated with high levels of miR-18a ($P < 0.01$).

miR-18a promotes cell growth, migration and invasion

Because the overexpression of miR-18a implied an oncogenic roles in NPC, we then wanted to elucidate whether miR-18a has an oncogenic effect on NPC. We performed *in vitro* and *in vivo* experiments to determine the roles of miR-18a in NPC development including the effects on cell growth, migration and invasion. miRNAs function was tested by transfecting NPC cells with miR-18a mimics or the inhibitors antagomiR-18a (2′-O-methyl-modified RNA oligonucleotides complementary to miR-18a sequences). Over-expression of miR-18a mimics obviously increased cell proliferation, migration and invasion. In contrast, the miR-18a inhibitor inhibited the growth and invasion of NPC cells (Figure 2A). The experiments were repeated in different NPC cell lines (5-8F and 6-10B; Supplementary Figure 1), available at *Carcinogenesis* Online). The wound-healing assay showed that miR-18a promoted the migration and mobility of HK1 cells. Over-expression of miR-18a using mimics clearly promoted wound gap closure in a time-dependent manner. Knocking down miR-18a using chemically synthesized miR-18a inhibitors delayed wound gap closure (Figure 2B). The transwell migration assay showed that miR-18a increased invasion ability. Representative figures of the migrated stained cells are shown. The cells in five randomly selected areas were counted and statistical analyses were performed using SPSS 11.0. The data are shown as the mean ± standard deviation (SD; Figure 2C, $*P < 0.05$; $**P < 0.01$, $***P < 0.001$; two-sided Student's *t*-test). The experiment was repeated in three NPC cell lines (HK1, 5-8F and 6-10B). The results of the other two cell lines are shown in Supplementary Figure 1, available at *Carcinogenesis* Online. Stable miR-18a over-expression and suppression in HK1 cells were established using lentivirus-based delivery. The expression of miR-18a in these stably transfected HK1 cells was verified using real-time PCR (Supplementary Figure 2, available at *Carcinogenesis* Online). The *in vivo* roles of miR-18a in cell growth and migration were assessed through tumour formation following subcutaneous or intravenous injection into nude mice with HK1 cells that had miR-18a either stably over-expressed or suppressed. The nude mice formed larger subcutaneous tumours in mice receiving cells over-expressing miR-18a compared with the control group ($n = 4$–5/group; $P = 0.02$, ANOVA, Figure 2D). The mobility and metastasis of cells *in vivo* were examined using the IVIS imaging system (Xenogen) at different time points after the intravenous injection. High luciferase activity was observed in the lung and long bone in the mice receiving the cells over-expressing miR-18a, whereas reduced luciferase activity was observed in the miR-18a-suppressed group ($n = 5$/group; $P < 0.05$, ANOVA, Figure 2E). The lungs with metastases were resected and processed for haematoxylin and eosin staining. As shown in Figure 2E-III, miR-18a over-expression increased the metastatic colonization.

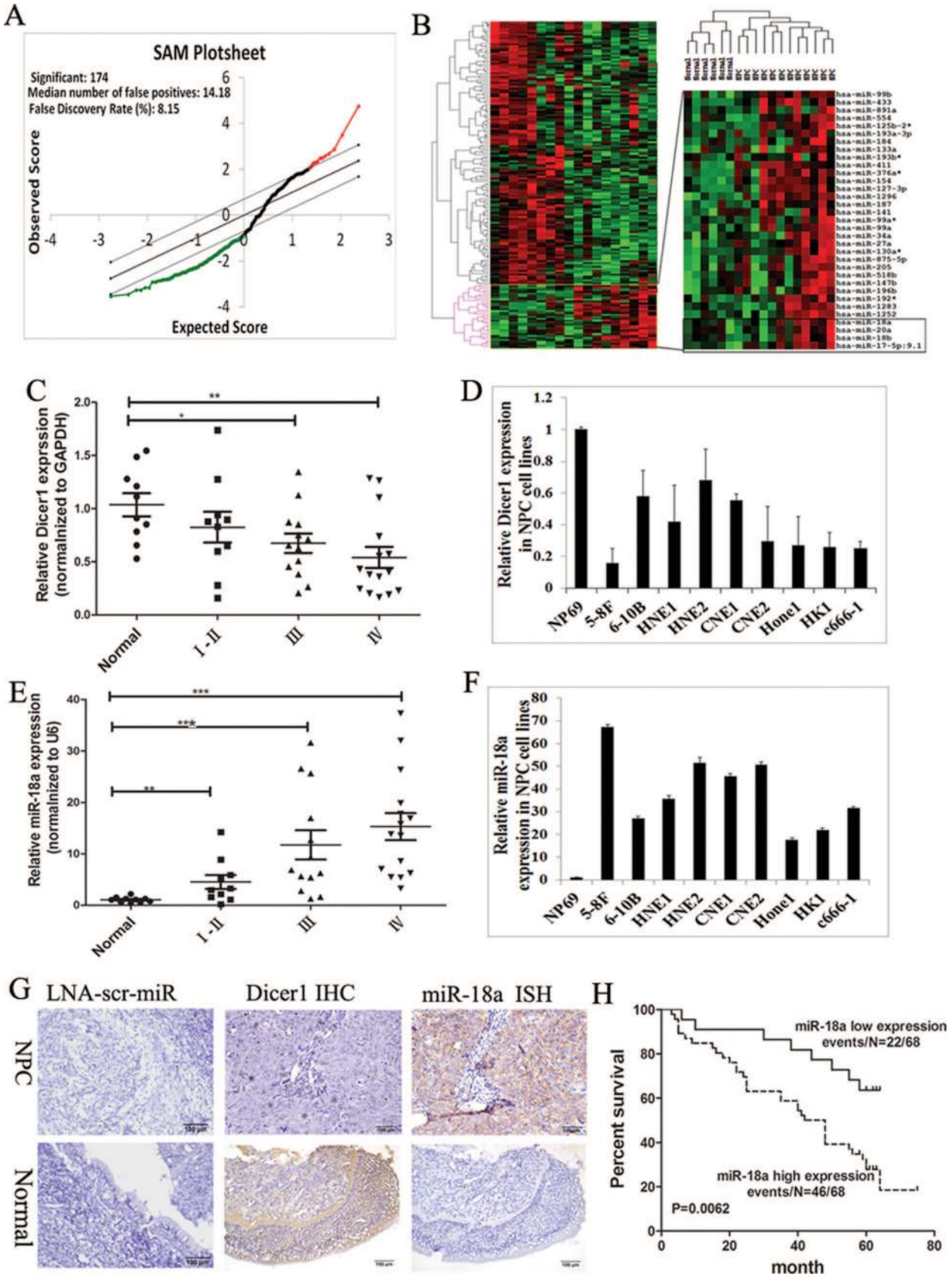

Fig. 1. Evaluation of the miRNA expression profiles from NPC samples revealed the global repression of miRNA expression. (**A**) The miRNA microarray analysis showed that 174 miRNAs were differentially expressed between NPC samples and healthy control nasopharyngeal samples. The SAM plot sheet identified the significantly differentially expressed miRNAs in the NPC samples. The scatter plot of the observed scores versus the expected scores is shown. The solid line indicated the line for observed scores = expected scores, where the observed relative difference was identical to the expected relative difference. The dotted lines are drawn at a distance $\Delta = 0.7$ from the solid line. The cutoff for 2-fold change is indicated by the dashed lines. The red, green and black dots

Table I. The correlation of clinical and pathological features with miR-18a expression in 168 NPC patients

Clinical and pathological features	miR-18a		χ^2	*P* value
	+High ≥8	–low <8		
Total (*n* = 168)				
Gender			0.014	0.904
Men (127)	88	39		
Female (41)	28	13		
Age			0.639	0.424
≥50 (99)	66	33		
<50 (69)	50	19		
Lymph node metastasis			34.245	<0.001
Yes (109)	92	17		
No (59)	24	35		
Clinical stage			28.084	<0.001*
I–II (72)	34	38		
III–IV (96)	82	14		
EBV(VCA-IgA)			33.077	<0.001
≥1: 10+ (139)	109	30		
≤1: 10+ (29)	7	22		

*Comparing stage I–II with stage III–IV.

Dicer1 is a direct target of miR-18a and miR-18a plays oncogenic roles through Dicer1

Previous research has shown that Dicer1 is a potential target of miR-18a (8). The schematic diagram of miR-18a binding sites in the 3′ untranslated regions (UTR) of Dicer1 was shown in Figure 3A-I. To further verify the targeting of Dicer1 by miR-18a, reporter constructs in which the 3′ UTR of Dicer1, either wild type or mutant in the miR-18a binding sites, were cloned downstream of the luciferase open reading frame. miR-18a or control miRNA was cotransfected with the luciferase constructs. As shown in Figure 3A-II, transfection with miR-18a mimics led to a significant decrease in luciferase activity compared with the miRNA control. In contrast, luciferase activities of mutant 3′ UTR remained unchanged in miR-18a over-expressing cells. Furthermore, western blot analysis showed that over-expression of miR-18a suppressed the endogenous Dicer1 expression in the NPC cell lines HK1 and 5-8F, whereas blocking miR-18a resulted in upregulation of endogenous Dicer1 expression (Figure 3B).

We then investigated whether the oncogenic roles of miR-18a were dependent on Dicer1 expression. We transfected a Dicer1 construct that is miRNA insensitive into the NPC cell line HK1 followed by transfection of the miR-18a mimics. Over-expression of Dicer1 was confirmed by western blot analysis (Supplementary Figure 3A, available at *Carcinogenesis* Online). The transfection of miRNA-insensitive Dicer1 notably decrease the promoting effect on cell viability, invasion and mobility induced by miR-18a, suggesting the promoting effect of miR-18a on NPC cell lines was dependent on Dicer1 (Figure 3C-I; Figure 3D). We also designed an shRNA that targeted Dicer1, which showed a potent inhibitory effect on Dicer1 expression (Supplementary Figure 3B, available at *Carcinogenesis* Online). When an miR-18a inhibitor was transduced into cells with knockdown of Dicer1, the miR-18a inhibitor did not show the anti-tumour effects shown above (Figure 3C-II; Figure 3E). These results supported the hypothesis that miR-18a executes an oncogenic effect on NPC cells, at least partly, through downregulating the expression of Dicer1.

We next investigated whether Dicer1 contributed to the development of NPC. Knockdown of Dicer1 in NPC cells resulted in clearly enhanced cell growth and cell mobility (Figure 3C-II; Figure 3E) by the upregulation of E-cadherin expression and downregulation of K-Ras expression levels (Figure 4B and 4E, lane 2). We then examined the regulatory roles of miR-18a on E-cadherin and K-Ras in HK1 cells. As shown in Figure 4A and 4D, we found that miR-18a downregulated the expression levels of E-cadherin and upregulated expression of K-Ras. The over-expression of miR-insensitive Dicer1 significantly reversed the expression patterns of the above molecules, which suggested that miR-18a regulates the expression levels through inhibition of Dicer1 expression (Figure 4B and 4E). In contrast, suppression of miR-18a resulted in clear upregulation of E-cadherin expression and downregulation of K-Ras expression, which were predicted to be the consequence of Dicer1 upregulation. The lentivirus-mediated knockdown of Dicer1 reversed the effects of antogomiR-18a, suggesting that miR-18a affected the expression of E-cadherin and K-Ras through the regulation of Dicer1 (Figure 4C and 4F).

Using the qRT–PCR, we found that miR-18a significantly downregulated the expression levels of E-cadherin and upregulated the expression levels of vimentin, ZEB1, ZEB2 and fibronectin, which are the markers indicative of epithelial mesenchymal transition (EMT). This regulatory effect was dependent on Dicer1 (Figure 4G–K). Consistent with the molecular changes, the cells' morphology after over-expression of miR-18a also showed the change of epithelial-like cells into fibroblast-like cells (Figure 4M). The fluorescent immunohistochemistry of E-cadherin also confirmed that over-expression of miRNA-18a mimics reduced the expression of E-cadherin (Figure 4N).

The global downregulations of miRNAs by miR-18a through Dicer

As the biogenesis of miRNA depends on cleavage by the ribonuclease III enzyme Dicer, miR-18a may change miRNA expression profiles by targeting Dicer1. We therefore performed an miRNA microarray

←
represented upregulated, downregulated and unchanged miRNAs, respectively. From the SAM plot sheet, the number of significantly upregulated miRNAs was 33, and the number of significantly downregulated miRNAs was 141 with a false discovery rate of 8.15%. (**B**) Unsupervised hierarchical clustering indicated the existence of two distinct branches: normal and cancer samples. The miRNA microarray analysis showed that 174 miRNAs were differentially expressed between NPC and normal control nasopharyngeal samples. The black box indicates the miR-17–92 cluster that was upregulated in NPC samples. The samples are in columns; the miRNAs are in rows. The raw data are shown in NCBI, GEO:GSE32906. (**C**) Real-time RT–PCR analysis of Dicer1 was performed in 38 NPC and 10 control normal nasopharyngeal samples. The comparative Ct ($2^{\Delta\Delta Ct}$) method was used to determine the fold change in the expression levels of Dicer1. The expression was normalized to human GAPDH. The expression of Dicer1 was lower in different NPC stages compared with normal counterparts. The data are shown as the mean ± standard error mean (*$P < 0.05$; **$P < 0.01$; ***$P < 0.001$, two-sided Student's *t*-test). (**D**) Real-time RT–PCR analysis of Dicer1 was performed in the NPC cell lines and the immortalized nasopharyngeal epithelial cells NP69. The expression was normalized to human GAPDH. The expression of Dicer1 was lower in NPC cell lines compared with the nasopharyngeal epithelial cells NP69. The data are presented as rhe mean ± SD of three replicates. (**E**) Validation of microarray data was performed using real-time RT–PCR. Real-time RT–PCR analysis of miR-18a was performed in the above-mentioned 38 NPC and 10 control normal nasopharyngeal samples. The comparative Ct ($2^{\Delta\Delta Ct}$) method was used to determine the fold change in the expression of miR-18a. The expression was normalized to human U6 snRNA. Expression of miR-18a was higher in different NPC stages compared with the normal counterparts. The data are shown as the mean ± standard error mean (*$P < 0.05$; **$P < 0.01$; ***$P < 0.001$, two-sided Student's *t*-test). (**F**) Real-time RT–PCR analysis of miR-18a was performed in NPC cell lines and the immortalized nasopharyngeal epithelial cell lines NP69. Compared with the immortalized nasopharyngeal epithelial cells NP69, the expression of miR-18a was clearly upregulated in the NPC cell lines including 5-8F, 6-10B, HNE1, CNE1, CNE2, HONE1, HK1 and C666-1. The expression of miR-18a was normalized to U6. The data are presented as the mean ± SD of 3 replicates. (**G**) Dicer1 and miR-18a were detected in NPC samples and in normal nasopharyngeal epithelial tissues. The samples were embedded in paraffin wax. The sections were incubated with anti-Dicer1 antibody. Representative images are shown (100 X). The expression of miR-18a was measured using *in situ* hybridization in NPC and normal nasopharyngeal epithelial tissues. Haematoxylin and eosin stains were used to counterstain. LNA-scr-miR was used as a negative control probe. Representative images are shown (100 X). (**H**) Kaplan–Meier curves are shown for patients according to tumour expression of miR-18a. The differences among the survival curves are shown. NPC death was significantly associated with the expression of miR-18a. Lower overall patient survival ($n = 68$) was associated with higher expression of miR-18a ($P < 0.01$).

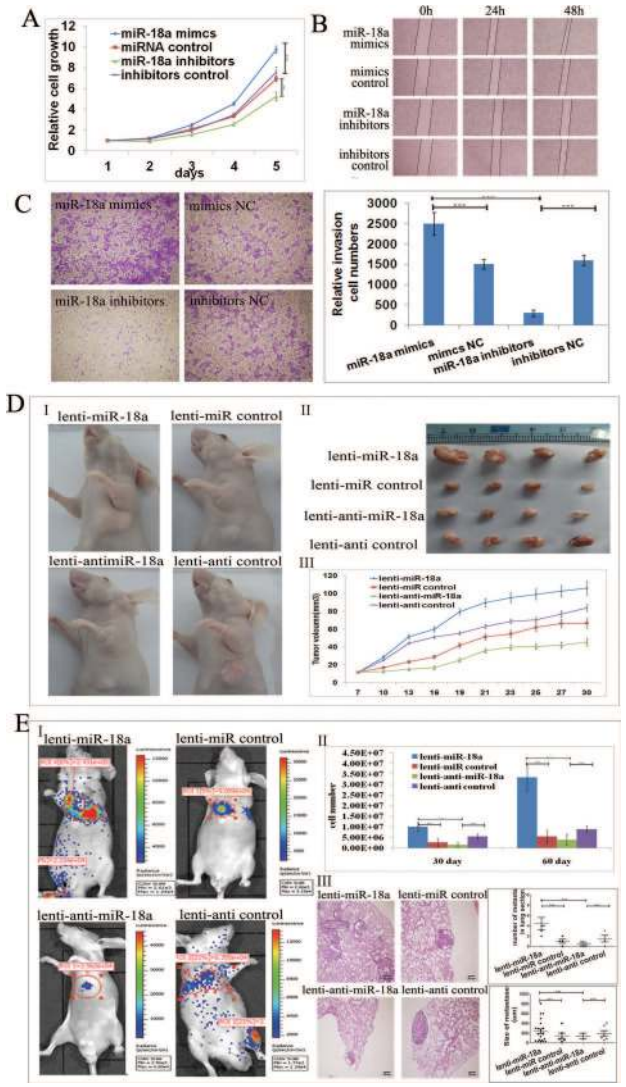

Fig. 2. miR-18a promoted tumour cell growth and invasion *in vitro*. (A) miR-18a promoted tumour cell growth. The MTT cell viability assay showed that miR-18a increased cell viability. The MTT assay was performed after transfection of miR-18a mimics or miR-18a inhibitor into the NPC cell lines HK1. Over-expression of miR-18a resulted in evident proliferation of HK1. The miR-18a inhibitor significantly inhibited the growth of HK1 cells. The data represent the mean values of three experiments, each performed in triplicates. The data are shown as the mean ± SD. (B) miR-18a promoted tumour cell invasion *in vitro*. The wound-healing assay showed that miR-18a promoted the migration and mobility of HK1 cells. Overexpression of miR-18a using mimics clearly promoted wound gap closure in a time-dependent manner. Knocking down miR-18a using chemically synthesized miR-18a inhibitors delayed wound gap closure. (C) The transwell migration assay showed that miR-18a increased invasion ability. Representative figures of the migrated stained cells are shown. The cells in five randomly selected areas were counted and statistical analyses were performed using SPSS 11.0. The data are shown as the mean ± SD. (*$P < 0.05$; **$P < 0.01$; ***$P < 0.001$; two-sided Student's *t*-test). The experiment was repeated in three NPC cell lines (HK1, 5-8F and 6-10B). The results of the other two cell lines are shown in Supplementary Figure 1, available at *Carcinogenesis* Online. (D). miR-18a promotes tumour cell growth and invasion *in vivo*. I: Nude mice were subcutaneously injected with lentivirus-mediated miR-18a-over-expressed or -suppressed of HK1 cells. II: The tumours excised from the mice are shown. III: The tumours were measured every 3 days, and the growth curves were plotted for each group. The tumour volumes were estimated using the following formula: length × width^2 × 0.52. Tumour growth was clearly increased in the miR-18a-over-expressing HK1 group (n = 4–5/group, $P < 0.01$, ANOVA). (E) miR-18a promoted metastasis dissemination *in vivo*. Nude mice were intravenously injected in the tail vein with lentivirus-mediated miR-18a-over-expressed or -suppressed of HK1 cells. The HK1 cells also stably expressed GFP-luciferase. I: The IVIS imaging system was used to monitor the migration of luciferase-labelled HK1 cells *in vivo*. High luciferase activity was observed in the lung and long bone in the mice receiving the cells overexpressing miR-18a, whereas reduced luciferase activity was detected in the miR-18a-suppressed group. Representative bioluminescent images are shown. II: Histograms depict the number of luciferase-positive cells in the selected region. Bioluminescence values were calculated by measuring photons/s/cm 2 /sr in the region of interest. The cell numbers were calculated from the standard curve (n = 4–5/group; $P < 0.01$, ANOVA). III: Representative images are shown of haematoxylin and eosin staining of lung sections. Haematoxylin and eosin staining was performed to detect the metastatic nodules in the lung. Over-expression of miR-18a increased the metastatic colonization. Black dotted circles indicate the metastatic foci. The scatter diagram depicts the number of metastatic nodules in 4–5 slides from every group. The size of the metastatic nodules was calculated from the diameters estimated using reticule equipped in the microscope.

assay to investigate the changes in miRNA profiles caused by miR-18a. The results showed the over-expression of miR-18a globally caused a downregulation of miRNA expression (671 of all of 858 miRNAs; GEO:GSE32680; Figure 5A). Furthermore, the global downregulation of miRNAs was restored by over-expression of miR-insensitive Dicer1 (GEO:GSE32680; Figure 5B). We then validated several miRNA expression levels using qRT–PCR. The downregulated expression levels of selected miRNAs including miR-29a/b, miR-200a/b/c, miR-429, miR-34b/c, miR-99a, miR-143 and miR-181 induced by miR-18a over-expression were confirmed, and the miR-18a inhibitor upregulated the expression levels of these miRNAs (Figure 5C). Among the miRNAs that were downregulated by miR-18a, we were interested in the roles of the miR-200 family and miR-143. The miR-18a mimics downregulated the miR-200 family and miR-143, whereas the miR-insensitive Dicer1 over-expression in turn reversed the downregulation, further confirming the effect of miR-18a on the biogenesis of global miRNAs via the targeting of Dicer1 (Figure 5D). Previously, it was shown that E-cadherin was repressed by ZEB1 and ZEB2, which are the target genes of the miR-200 family (33), and K-Ras was identified as a target gene of miR-143 (34). We then investigated whether the regulatory effect of miR-18a on the expression of E-cadherin and K-Ras was dependent on miR-200 and miR-143. miR-18a transfection downregulated the expression of E-cadherin, whereas additional transfection of the miR-200 family rescued the inhibitory effect of miR-18a on the expression of E-cadherin. miR-18a upregulated the expression of K-Ras and additional transfection of miR-143 reversed the enhanced effect of miR-18a on the expression of K-Ras (Figure 5E–H). These results indicated that the oncogenic roles of miR-18a were partly through influencing the biogenesis of miRNome.

Discussion

A global downregulation of miRNA levels is among the most common molecular alterations in cancer, and this downregulation was also observed in NPC samples (23,24). It is worth noting that certain miRNAs are upregulated in cancer; generally, the miRNAs that are upregulated in cancer have oncogenic properties. Notably, the upregulated miRNAs that target Dicer1 may alter the overall biogenesis of miRNAs, resulting in the progression of cancer through a complex interaction of miRNAs and their downstream target genes, and the feedback loop certainly increases the complexity of the miRNA profiles. Among the upregulated miRNAs resulting from the miRNA array of NPC samples (NCBI, GEO:GSE32906), miR-18a/b were predicted to target the 3′ UTR of Dicer1. miR-18a was confirmed to target the Dicer 3′ UTR using luciferase activity and western blot assays. Over-expression of miR-18a resulted in the overall downregulation of miRNAs (78%), which could be restored by the forced expression of Dicer. Verified by functional studies such as MTT, migration and tumour formation assays *in vitro* and *in vivo*, miR-18a was shown to function as a master regulator of the miRNAs that target the process of miRNAs biogenesis: alters overall expression levels of miRNAs and

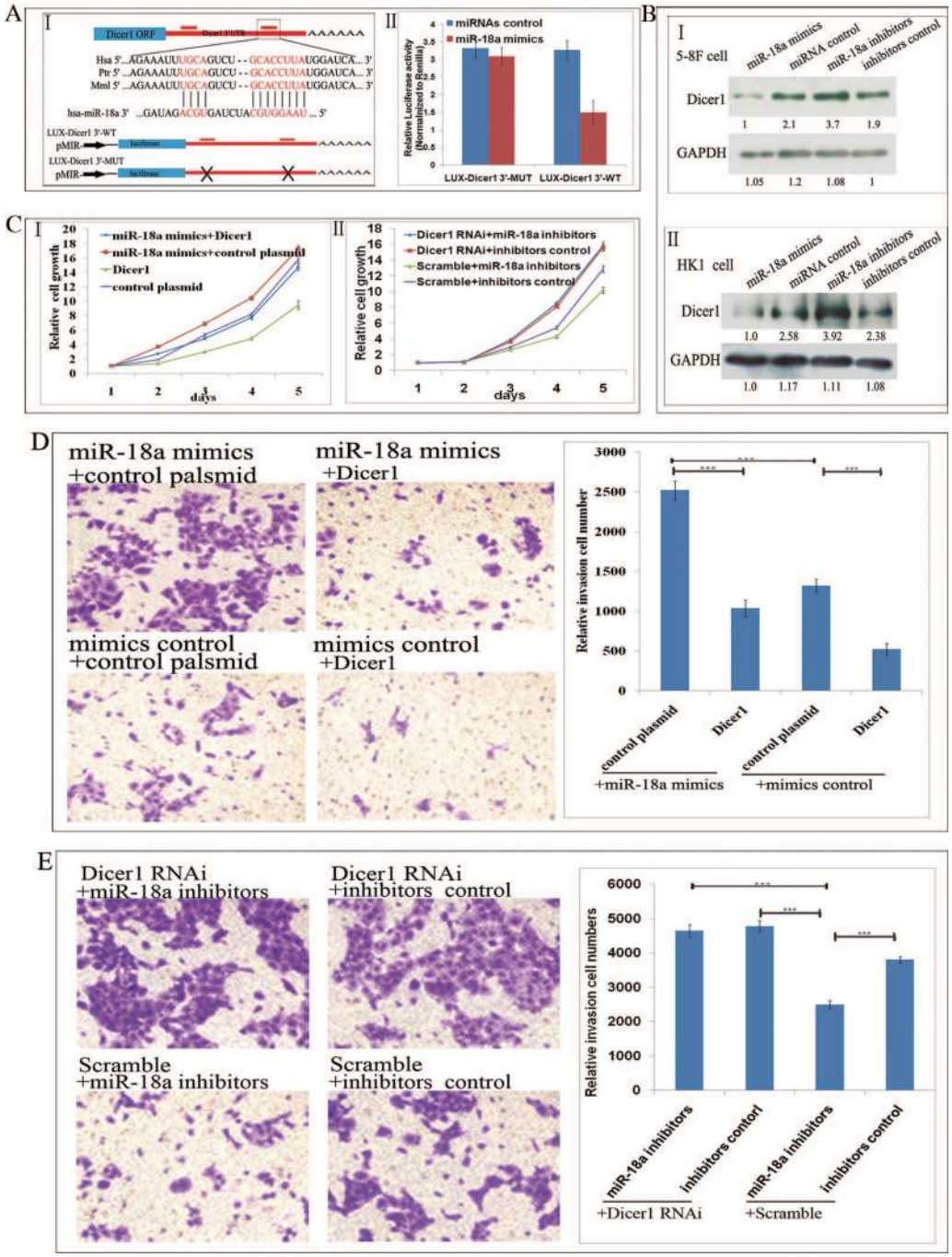

Fig. 3. Dicer1 is a direct target gene of miR-18a. (**A**) I: A schematic representation of the 3′ UTR of Dicer1. The red bars show the predicted miR-18a binding sites in the 3′ UTR of Dicer1. The mature miR-18a sequence aligned to the target sites is shown. The evolutionary conservation in the seed sequence between Pan troglodjaes (Ptr), Mouse (Mmu) and Human (Hsa) is shown in red highlights. II: Luciferase activity assay. The reporter constructs are shown in which the 3′ UTR of Dicer with either wild-type or mutant (LUX-Dicer 3′-WT or LUX-Dicer 3′-MUT) miR-18a binding sites was cloned downstream of the luciferase open reading frame. HK1 cells were co-transfected with the luciferase construct and miR-18a mimics or control miRNA. The Renilla construct was also co-transfected as an internal control. Luciferase activity was normalized to Renilla luciferase activity. The data are presented as the mean ± SD of two experiments with six replicates each (Student *t*-test, $*P < 0.05$; $**P < 0.01$; $***P < 0.001$). (**B**) miR-18a downregulated the expression of Dicer1. Western blot analyses of Dicer1 were performed 48 h after transfection of the miR-18a mimics and the miR-18a inhibitor (2′-O-methyl-modified RNA oligonucleotides complementary to miR-18a sequences). GAPDH was used as an internal control. These experiments were repeated in different NPC cell lines, I: HK1; II: 5-8F. (**C**) miR-18a promoted cell growth and migration *in vitro* through Dicer1. I: The MTT cell viability assay showed that miR-18a promoted cell viability through Dicer1. An MTT assay was performed after cotransfection of the miR-18a mimics and the Dicer1 construct or control plasmid into the NPC cell line HK1. Dicer 1 transfection reduced the cell proliferation induced by miR-18a. The data represent the mean values of three experiments, each performed in triplicates. The data are shown as the mean ± SD. II: An MTT assay was performed after cotransfection of the miR-18a inhibitor and the Dicer1 RNAi construct or scramble into the NPC cell line HK1. The growth-suppressive effect of the miR-18a inhibitor was clearly attenuated when endogenous Dicer1 was knocked down. The data represent the mean values of three experiments, each performed in triplicates. The data are shown as the mean ± SD. (**D**) Transwell migration assays showed that miR-18a increased cell invasive ability through Dicer1. Representative figures show the stained, migrated cells. Dicer1 transfection clearly reduced the cell invasion induced by miR-18a. (**E**) Transwell migration assays showed that the transfection of the miR-18a inhibitor clearly reduced the number of migrated cells, but the knockdown of endogenous Dicer1 partly reversed the inhibitory effect of miR-18a. The cells in five randomly selected areas were counted and statistical analyses were performed using SPSS 11.0. The data are shown as the mean ± SD. ($*P < 0.05$; $**P < 0.01$; $***P < 0.001$; two-sided Student's *t*-test).

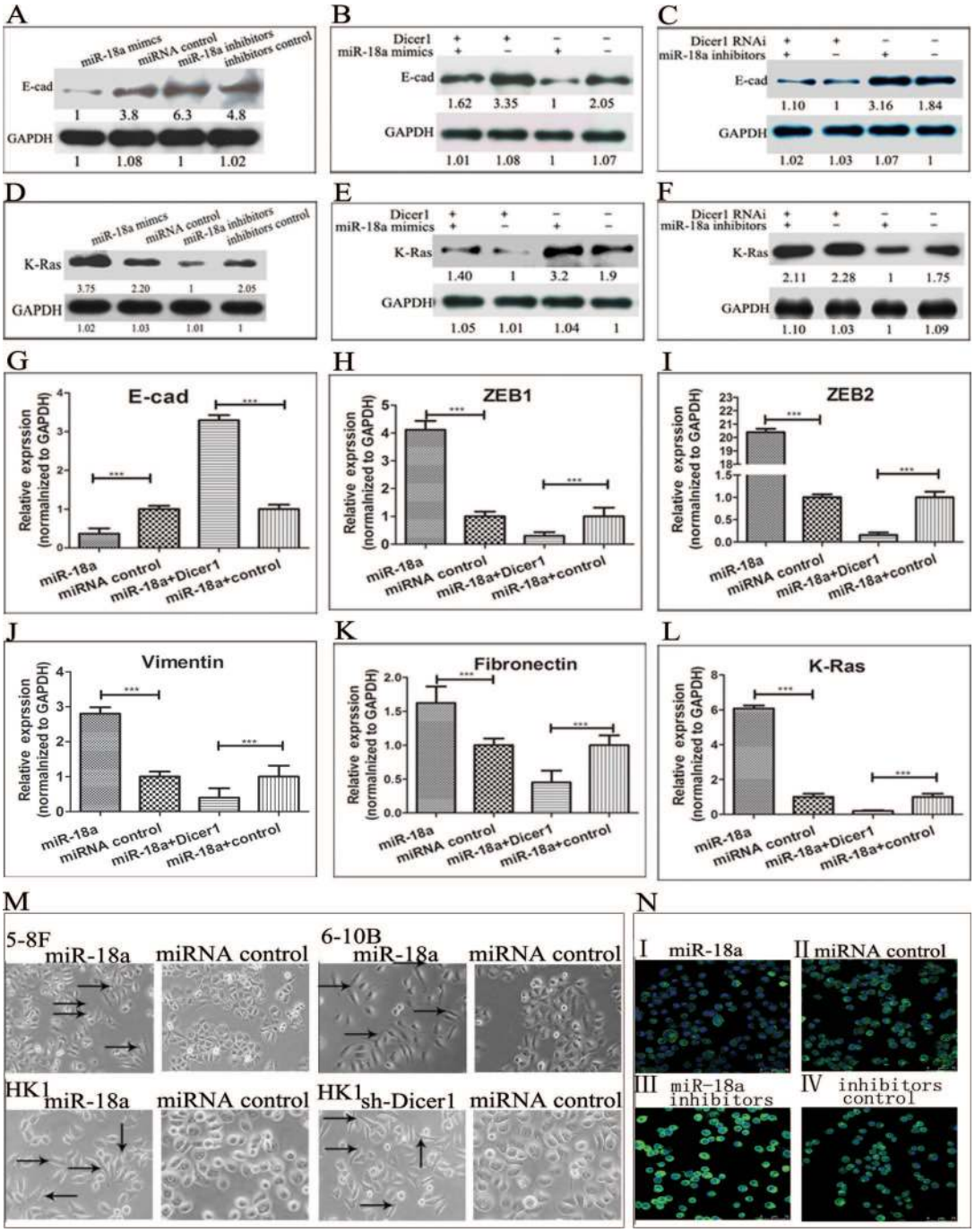

Fig. 4. Dicer1 is involved in the miR-18a-induced expression changes of E-cadherin and K-Ras in HK1 cells. (**A**) miR-18a downregulated the expression of E-cadherin. Transfection of miR-18a mimics caused the downregulated expression of E-cadherin compared with the miRNA control. miR-18a inhibitor caused the upregulation of E-cadherin. (**B**) miR-18a downregulated the expression of E-cadherin through Dicer1. miR-18a induction alone downregulated the expression of E-cadherin (lane 3), whereas cotransfection of miR-18a and Dicer1 partly reverse the inhibitory effect on expression of E-cadherin (lane 1). (**C**) miR-18a inhibitor upregulated the expression of E-cadherin (lane 3), whereas knockdown of Dicer1 led to a reduction in the effect of the miR-18a inhibitor (lane 1). (**D**) miR-18a upregulated the expression of K-Ras. Transfection of miR-18a mimics upregulated the expression of oncogenic K-Ras and miR-18a inhibitor clearly downregulated the expression of K-Ras. (**E**) miR-18a upregulated the expression of K-Ras through Dicer1. miR-18a induction alone upregulated the expression of K-Ras (lane 3), whereas cotransfection of miR-18a and Dicer1 partly rescued miR-18a-induced overexpression of K-Ras (lane 1). (**F**) The miR-18a inhibitor downregulated the expression of K-Ras (lane 3), whereas knockdown of Dicer1 partly reversed effect of the miR-18a inhibitor (lane 1). Densitometer tracing values of each band are shown. A GAPDH antibody was used to normalize the densitometer values to account for differences in loading and transfer efficiencies. (**G–K**) Quantitative RT–PCR showed that miR-18a significantly downregulated the expression of E-cadherin and upregulated the expression of vimentin, ZEB1, ZEB2 and fibronectin, which are the markers indicative of the EMT. Dicer1 rescued the exprssion of E-cadherin and downregulated the expression of vimentin, ZEB1, ZEB2 and fibronectin. (**L**): Quantitative RT–PCR showed that miR-18a significantly upregulated the expression of K-Ras. Dicer1 reversed the overexpression of K-Ras. PCR quantification used the ΔΔCt method against GAPDH for normalization. The data are representative of the means of three experiments. The bars represent the relative expression change compared with the negative control. (**M**) Transfection of miR-18a mimics led to the morphologic change of epithelial-like cells into the fibroblast-like cells. The arrow indicates the fibroblast-like cells (200 X). (**N**): An immunofluorescent assay was performed to detect the expression of E-cadherin; representative fields are shown. The sections were incubated with E-cadherin antibody. I: The miR-18a mimics clearly reduced E-cadherin expression on the HK1 cell surface, whereas the miR-18a inhibitor enhanced E-cadherin expression on the HK1 cell surface (III).

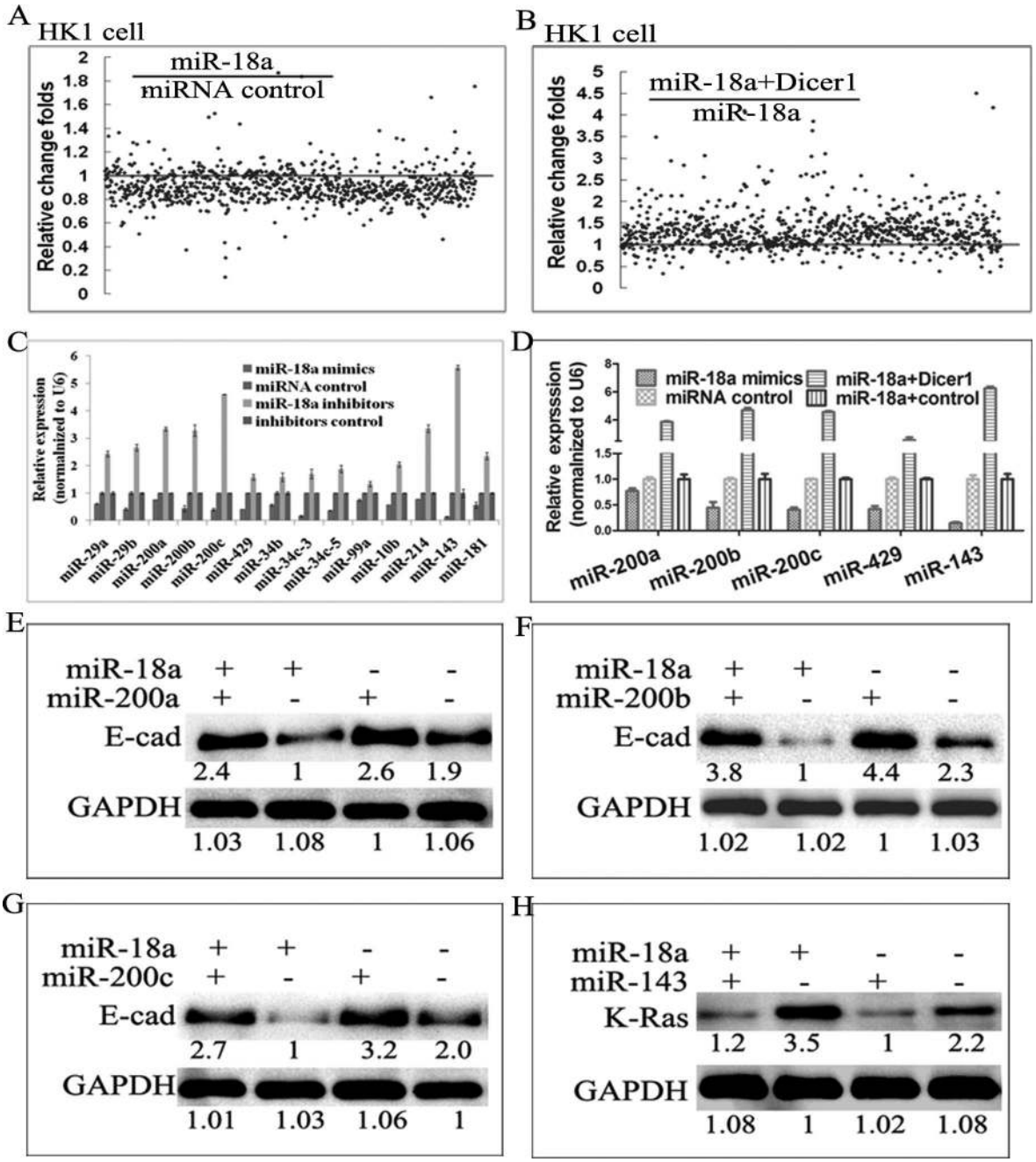

Fig. 5. The miRNA profile changes induced by miR-18a. The Illumina microRNA Expression Profiling Assay was performed to evaluate the changes in the miRNA profiles after miR-18a induction. (A) The over-expression of miR-18a caused globally downregulated expression of miRNAs. The dots indicate the ratio of miRNA expression value in miR-18a-transfected cells and control miRNA-transfected cells. The data showed that 671 of all 858 miRNAs were downregulated after transfection with miR-18a mimics. (B) Dicer1 over-expression restored the overall downregulated miRNAs. Dicer1-forced expression in the miR-18a-transfected HK1 cells rescued the expression of most miRNA expression levels (692 of all 858 miRNAs). The dots indicate the ratio of miRNA expression value in miR-18a mimics-transfected HK1 cells versus co-transfection of miR-18a mimics and Dicer1 construct. (C) qRT–PCR was performed to confirm the selected miRNA expression. miR-18a over-expression resulted in the downregulated expression of several miRNAs including miR-29a/b, miR-200a/b/c, miR-429, miR-34b/c, miR-99a, miR-143 and miR-181. PCR quantification used the thCt method against U6 for normalization. The data are representative of the means of three experiments. (D) qRT–PCR was performed to confirm that miR-18a downregulated the expression of the miR-200 family and miR-143 by Dicer1. The transfection of miR-18a mimics caused the downregulated expression of miR-200 family and miR-143. Dicer1-forced expression rescued the expression of miR-200 family and miR-143. PCR quantification used the thCt method against U6 for normalization. The data are presented as the mean ± SD of three experiments. miR-18a downregulated the expression of E-cadherin through suppression of (E) miR-200a; (F) miR-200b and (G) miR-200c. Transfection of the miR-200 family rescued the inhibitory effect of miR-18a on the expression of E-cadherin. (H) miR-18a upregulated the expression of K-Ras through suppressing miR-143. Transfection of miR-143 reversed the promoting effect of miR-18a on the expression of K-Ras. Densitometer tracing values of each band are shown.

potentially affects key gene expression levels estimated to be regulated by miRNome.

miRNAs regulate the expression of hundreds of target genes. It is predicted that miRNAs preferentially interact with genes that are central to highly connected networks (35). miR-10b, miR-9 and members of miR-200 family have been reported to play critical roles in EMT or EMT-related events (36–38). One of the most striking types of metastasis initiation functions is the EMT. EMT occurs at the invasive front

of tumours whereby cells lose E-cadherin expression, detach, invade and break down the basement membrane. Our study demonstrated that miR-18a transduction drove morphogenetic changes through repression of the cell–cell adhesion protein E-cadherin. To elucidate the mechanisms of miR-18a-induced repression of E-cadherin, we verified the data obtained from the miRNA microarray showing that induction of miR-18a resulted in a global downregulation of miRNAs (Figure 5A and 5B). The selected miRNAs included miR-200 family, miR-143, miR-29a/b and miR-34b/c. The quantitative real-time PCR for individual miRNA were performed to verify miRNA expression levels after miR-18a transduction. miR-200a, miR-200b, miR-200c and miR-429, which are the members of the miR-200 family, were significantly downregulated by miR-18a expression. The reduced expression was reversed by forced Dicer1 expression, suggesting that miR-18a downregulates the expression of the miRNA-200 family through Dicer1 and implying a role for miR-18a in cancer metastasis. Notably, miR-143 was dramatically downregulated by miR-18a, as demonstrated by the miRNA array. The downregulation of miR-143 by miR-18a and the restored expression by Dicer1 was confirmed using quantitative real-time PCR. As K-Ras is a putative target gene of miR-143, miR-18a may modulate K-Ras through miR-143, which was confirmed using western blot analysis. From the data obtained, we presumed that miR-18a influences numerous genes involved in metastasis initiation, progression and colonization.

Most recently, we noticed the relationship of Dicer1 and NPC development. It was previously reported that miR-BART6-5p RNAs encoded by EBV genome silence Dicer1 through multiple target sites located in the 3′ UTR of Dicer1 mRNA (39). Our group found a significantly low expression level of Dicer1 in 251 NPC cases (31). The influence of Dicer1 in tumour cells has been studied with controversial results among different cancer types. In several types of cancers such as lung, breast and ovarian cancer, reduced expression levels of Dicer1 was observed and were associated with poor prognosis (40–43). However, in contrast, strong expression of Dicer predicted poor prognosis in patients with colorectal cancer and cutaneous melanoma (43,44). Another report showed that the mRNA levels of Dicer1 were significantly augmented in stage III compared with stage II tumours in colorectal cancer (45). In contrast, Dicer expression levels in liver metastases of colorectal cancer were decreased compared either normal mucosa or the primary tumour in both colon and rectal cancers (46). It appears that Dicer plays more important roles in the metastatic process of cancer. The discrepancies of Dicer1 expression levels in different cancer types require further exploration. Mutations in the *Dicer1* gene have been shown to be a common process underlying the different cancers. Hemizygous deletions of *Dicer1* accelerate tumour formation (47). The inconsistent results may be partly due to the different function of wild-type *Dicer1* and mutant *Dicer1*, although this hypothesis has not been verified.

Although several miRNAs are upregulated in specific tumours, a global reduction of miRNA abundance appears to be a general trait of human cancers (3,4). The present work demonstrated that miR-18a expression was associated with NPC growth and metastasis. Interestingly, miR-18a expression was substantially higher in ERα-negative than in ERα-positive breast cancer samples ($P < 0.0001$ (48)). Certain miRNAs, such as miR-222/221 and miR-29a, are dramatically higher in ESR1− cells (100- and 16-fold higher, respectively). miR-222/221 (which target ESR1 itself) and miR-29a are predicted to target the 3′ UTR of Dicer1. Addition of these miRNAs to ESR1+ cells reduces Dicer protein expression levels, whereas inhibition of miR-222 in ESR1− cells increases Dicer protein levels (49). It is possible that these upregulated miRNAs exert a cooperative function, mostly likely through Dicer.

In this study, miR-18a was able to promote cell growth and mobility, at least in part through targeting Dicer. The promoting effects could be reversed by the over-expression of Dicer. The immunohistochemistry and hybridization *in situ* strongly indicated the inverse correlation of Dicer expression and miR-18a expression. The clinical correlation analysis also confirmed the miR-18a was strongly indicative of poor progonoses and metastases.

Supplementary material

Supplementary Table 1 and Figures 1–3 can be found at http://carcin.oxfordjournals.org/

Funding

National Natural Science Foundation, China (81272255, 81000882, 91229122, 81172189); National Training and Research Base for Talents of Principles of Carcinogenesis Foundation (111 project: 111-2-12); Hunan Natural Science Foundation (10JJ7003).

Conflict of Interest statement: None declared.

References

1. Lu,J. *et al.* (2005) MicroRNA expression profiles classify human cancers. *Nature*, **435**, 834–838.
2. Ozen,M. *et al.* (2008) Widespread deregulation of microRNA expression in human prostate cancer. *Oncogene*, **27**, 1788–1793.
3. Kumar,M.S. *et al.* (2007) Impaired microRNA processing enhances cellular transformation and tumorigenesis. *Nat. Genet.*, **39**, 673–677.
4. Martello,G. *et al.* (2010) A MicroRNA targeting dicer for metastasis control. *Cell*, **141**, 1195–1207.
5. Huang,G. *et al.* (2012) miR-20a encoded by the miR-17-92 cluster increases the metastatic potential of osteosarcoma cells by regulating Fas expression. *Cancer Res.*, **72**, 908–916.
6. Yu,G. *et al.* (2012) Prognostic values of the miR-17–92 cluster and its paralogs in colon cancer. *J. Surg. Oncol*., **106:**232–237.
7. Hayashita,Y. *et al.* (2005) A polycistronic microRNA cluster, miR-17-92, is overexpressed in human lung cancers and enhances cell proliferation. *Cancer Res.*, **65**, 9628–9632.
8. Tao,J. *et al.* (2012) microRNA-18a, a member of the oncogenic miR-17-92 cluster, targets Dicer and suppresses cell proliferation in bladder cancer T24 cells. *Mol. Med. Report.*, **5**, 167–172.
9. Castellano,L. *et al.* (2009) The estrogen receptor-alpha-induced microRNA signature regulates itself and its transcriptional response. *Proc. Natl. Acad. Sci. U.S.A.*, **106**, 15732–15737.
10. Morimura,R. *et al.* (2011) Novel diagnostic value of circulating miR-18a in plasma of patients with pancreatic cancer. *Br. J. Cancer*., **105:**1733–1740.
11. Deng,M. *et al.* (2011) miR-216b suppresses tumor growth and invasion by targeting KRAS in nasopharyngeal carcinoma. *J. Cell. Sci.*, **124**(Pt 17), 2997–3005.
12. Alajez,N.M. *et al.* (2011) MiR-218 suppresses nasopharyngeal cancer progression through downregulation of survivin and the SLIT2-ROBO1 pathway. *Cancer Res.*, **71**, 2381–2391.
13. Lu,J. *et al.* (2011) MiR-26a inhibits cell growth and tumorigenesis of nasopharyngeal carcinoma through repression of EZH2. *Cancer Res.*, **71**, 225–233.
14. Ji,Y. *et al.* (2010) MiRNA-26b regulates the expression of cyclooxygenase-2 in desferrioxamine-treated CNE cells. *FEBS Lett.*, **584**, 961–967.
15. Li,G. *et al.* (2010) MicroRNA-10b induced by Epstein-Barr virus-encoded latent membrane protein-1 promotes the metastasis of human nasopharyngeal carcinoma cells. *Cancer Lett.*, **299**, 29–36.
16. Wong,T.S. *et al.* (2011) MicroRNA let-7 suppresses nasopharyngeal carcinoma cells proliferation through downregulating c-Myc expression. *J. Cancer Res. Clin. Oncol.*, **137**, 415–422.
17. Zhang,L. *et al.* (2010) microRNA-141 is involved in a nasopharyngeal carcinoma-related genes network. *Carcinogenesis*, **31**, 559–566.
18. Xia,H. *et al.* (2010) miR-200a-mediated downregulation of ZEB2 and CTNNB1 differentially inhibits nasopharyngeal carcinoma cell growth, migration and invasion. *Biochem. Biophys. Res. Commun.*, **391**, 535–541.
19. Wong,A.M. *et al.* (2012) Profiling of Epstein-Barr virus-encoded microRNAs in nasopharyngeal carcinoma reveals potential biomarkers and oncomirs. *Cancer*, **118:**698–710.
20. Barth,S. *et al.* (2011) EBV-encoded miRNAs. *Biochim. Biophys. Acta*, **1809**, 631–640.
21. Chen,S.J. *et al.* (2010) Characterization of Epstein-Barr virus miRNAome in nasopharyngeal carcinoma by deep sequencing. *PLoS One*, **5**, e12745.
22. Du,Z.M. *et al.* (2011) Upregulation of MiR-155 in nasopharyngeal carcinoma is partly driven by LMP1 and LMP2A and downregulates a negative prognostic marker JMJD1A. *PLoS ONE*, **6**, e19137.
23. Li,T. *et al.* (2011) microRNA expression profiling of nasopharyngeal carcinoma. *Oncol. Rep.*, **25**, 1353–1363.

24. Chen,H.C. *et al.* (2009) MicroRNA deregulation and pathway alterations in nasopharyngeal carcinoma. *Br. J. Cancer*, **100**, 1002–1011.
25. Sengupta,S. *et al.* (2008) MicroRNA 29c is down-regulated in nasopharyngeal carcinomas, up-regulating mRNAs encoding extracellular matrix proteins. *Proc. Natl. Acad. Sci. U.S.A.*, **105**, 5874–5878.
26. Luo,Z. *et al.* (2012) An in silico analysis of dynamic changes in microRNA expression profiles in stepwise development of nasopharyngeal carcinoma. *BMC Med. Genom.*, in press.
27. Bergeron,L. Jr *et al.* (2010) Short RNA duplexes guide sequence-dependent cleavage by human Dicer. *RNA*, **16**, 2464–2473.
28. Jakymiw,A. *et al.* (2010) Overexpression of dicer as a result of reduced let-7 MicroRNA levels contributes to increased cell proliferation of oral cancer cells. *Genes. Chromosomes Cancer*, **49**, 549–559.
29. Chiosea,S. *et al.* (2006) Up-regulation of dicer, a component of the MicroRNA machinery, in prostate adenocarcinoma. *Am. J. Pathol.*, **169**, 1812–1820.
30. Merritt,W.M. *et al.* (2008) Dicer, Drosha, and outcomes in patients with ovarian cancer. *N. Engl. J. Med.*, **359**, 2641–2650.
31. Guo,X. *et al.* (2012) The microRNA-processing enzymes: Drosha and Dicer can predict prognosis of nasopharyngeal carcinoma. *J. Cancer Res. Clin. Oncol*., **138:**49–56.
32. Xiang,J. *et al.* (2009) Mesenchymal stem cells as a gene therapy carrier for treatment of fibrosarcoma. *Cytotherapy*, **11**, 516–526.
33. Park,S.M. *et al.* (2008) The miR-200 family determines the epithelial phenotype of cancer cells by targeting the E-cadherin repressors ZEB1 and ZEB2. *Genes Dev.*, **22**, 894–907.
34. Chen,X. *et al.* (2009) Role of miR-143 targeting KRAS in colorectal tumorigenesis. *Oncogene*, **28**, 1385–1392.
35. Dans Devita,V.T. Jr *et al.* (2011) *Cancer: Principles & Practice of Oncology.* Wolters Kluwer, Lippincott Williams & Wilkins, Philadelphia. pp.160.
36. Ma,L. *et al.* (2007) Tumour invasion and metastasis initiated by microRNA-10b in breast cancer. *Nature*, **449**, 682–688.
37. Gregory,P.A. *et al.* (2008) The miR-200 family and miR-205 regulate epithelial to mesenchymal transition by targeting ZEB1 and SIP1. *Nat. Cell Biol.*, **10**, 593–601.
38. Korpal,M. *et al.* (2008) The miR-200 family inhibits epithelial-mesenchymal transition and cancer cell migration by direct targeting of E-cadherin transcriptional repressors ZEB1 and ZEB2. *J. Biol. Chem.*, **283**, 14910–14914.
39. Iizasa,H. *et al.* (2010) Editing of Epstein-Barr virus-encoded BART6 microRNAs controls their dicer targeting and consequently affects viral latency. *J. Biol. Chem.*, **285**, 33358–33370.
40. Karube,Y. *et al.* (2005) Reduced expression of Dicer associated with poor prognosis in lung cancer patients. *Cancer Sci.*, **96**, 111–115.
41. Yan,M., *et al.* (2012) Dysregulated expression of Dicer and Drosha in breast cancer. *Pathol. Oncol. Res.*, **18:**343–348.
42. Pampalakis,G. *et al.* (2010) Down-regulation of dicer expression in ovarian cancer tissues. *Clin. Biochem.*, **43**, 324–327.
43. Faber,C. *et al.* (2011) Overexpression of Dicer predicts poor survival in colorectal cancer. *Eur. J. Cancer*, **47**, 1414–1419.
44. Ma,Z. *et al.* (2011) Up-regulated Dicer expression in patients with cutaneous melanoma. *PLoS ONE*, **6**, e20494.
45. Papachristou,D.J. *et al.* (2011) Expression of the ribonucleases Drosha, Dicer, and Ago2 in colorectal carcinomas. *Virchows Arch.*, **459**, 431–440.
46. Stratmann,J. *et al.* (2011) Dicer and miRNA in relation to clinicopathological variables in colorectal cancer patients. *BMC Cancer*, **11**, 345.
47. Lambertz,I. *et al.* (2010) Monoallelic but not biallelic loss of Dicer1 promotes tumorigenesis *in vivo*. *Cell Death Differ.*, **17**, 633–641.
48. Yoshimoto,N. *et al.* (2011) Distinct expressions of microRNAs that directly target estrogen receptor α in human breast cancer. *Breast Cancer Res. Treat.*, **130**, 331–339.
49. Cochrane,D.R. *et al.* (2010) MicroRNAs link estrogen receptor alpha status and Dicer levels in breast cancer. *Horm. Cancer*, **1**, 306–319.

Received May 17, 2012; revised October 3, 2012; accepted October 14, 2012